iScience, Volume *24*

Supplemental information

Replication protein A plays multifaceted roles complementary to specialized helicases in processing G-quadruplex DNA

Yi-Ran Wang, Ting-Ting Guo, Ya-Ting Zheng, Chang-Wei Lai, Bo Sun, Xu-Guang Xi, and Xi-Miao Hou

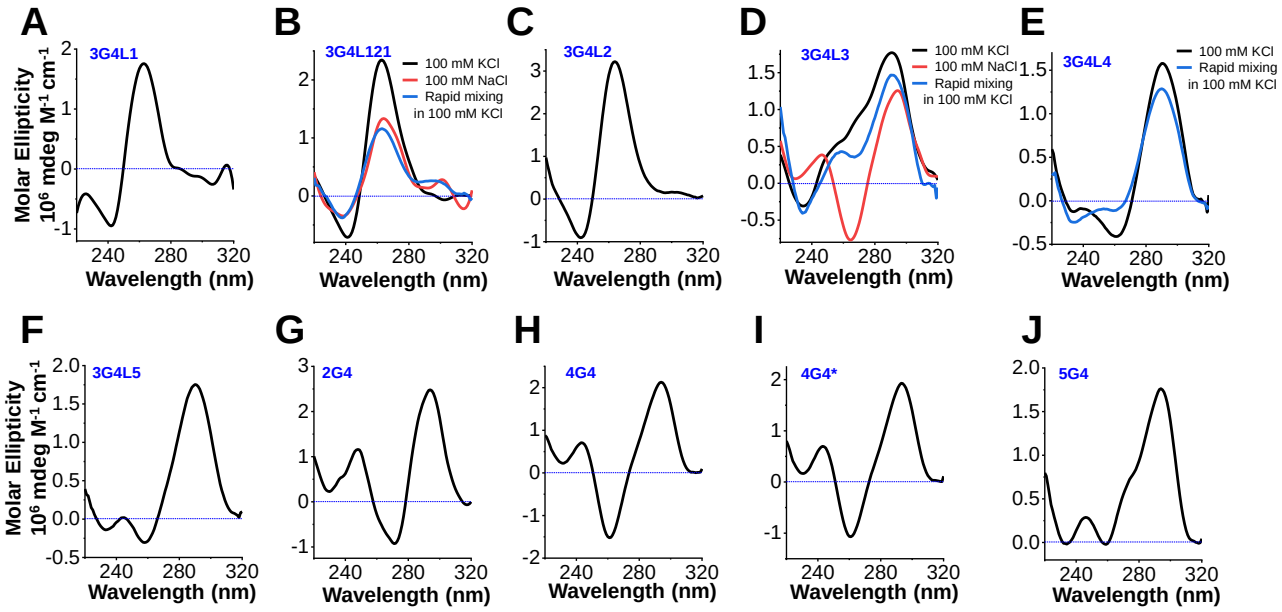

Figure S1. CD spectra confirm the formation of G4 structures. Related to Figure 1. The G4 structures were prepared by incubating the G4 sequences in 100 mM KCl (black) or 100 mM NaCl (red) at 95°C for 5 min and then slowly cooled down to room temperature in about 7 hours. Short-looped G4s including 3G4L1, 3G4L121, and 3G4L2 all adopt parallel topology. Long-looped G4s usually display the antiparallel or hybrid topology. In Figure S1B, S1D, and S1E, the curves in blue color were obtained by directly diluting the G4 sequences in 100 mM KCl without the above slow annealing procedure. In this condition, G4 structures can also be formed.

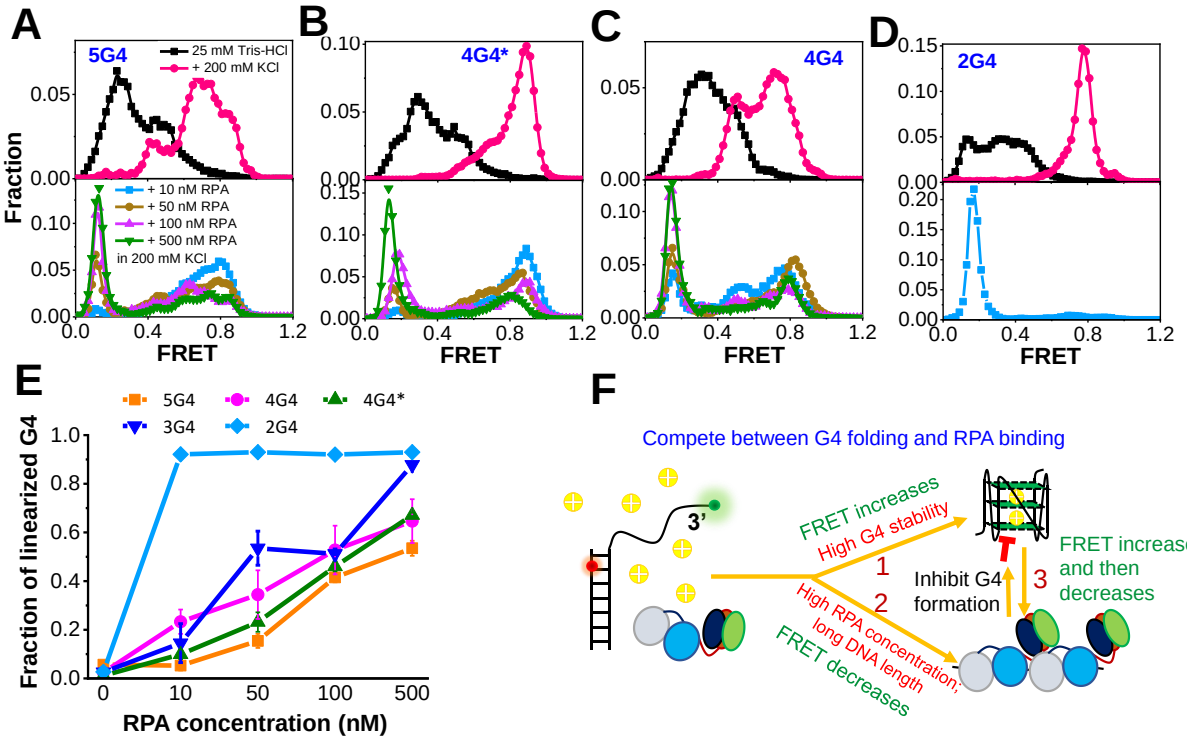

Figure S2. The inhibitory effects of RPA on the folding of G4 structures with varied G-tetrad layers. Related to Figure 1. (**A-D**) The upper panels are the FRET distributions of a series of G4 motifs in 25 mM Tris-HCl before and 4 min after the addition of 200 mM KCl, 5 mM $MgCl_2$. The lower panels are their FRET distributions after the addition of 10-500 nM RPA in the buffer containing 200 mM KCl, 5 mM $MgCl_2$. (**E**) The fractions of linearized G4s at the varied concentrations of RPA obtained from the FRET peaks at ~$E_{0.2}$. 3G4 represents the 3G4L3 in Figure 1H. The error bars were obtained from at least three repetitive experiments. Data are presented as mean±SEM. (**F**) The proposed mechanism of G4 folding in the presence of RPA. In the presence of RPA in KCl, G4s with low energy barriers may fold at a very fast rate (pathway 1). On the other hand, the preemptive binding of RPA onto ssDNA is more favored at high RPA concentration and with the long G4 sequence, resulting in the rapid ssDNA linearization (pathway 2). In addition, the association of RPA may also lead to the disruption of some temporarily folded G4s (pathway 3). However, the stable coating of ssDNA by RPA ultimately prevents its folding.

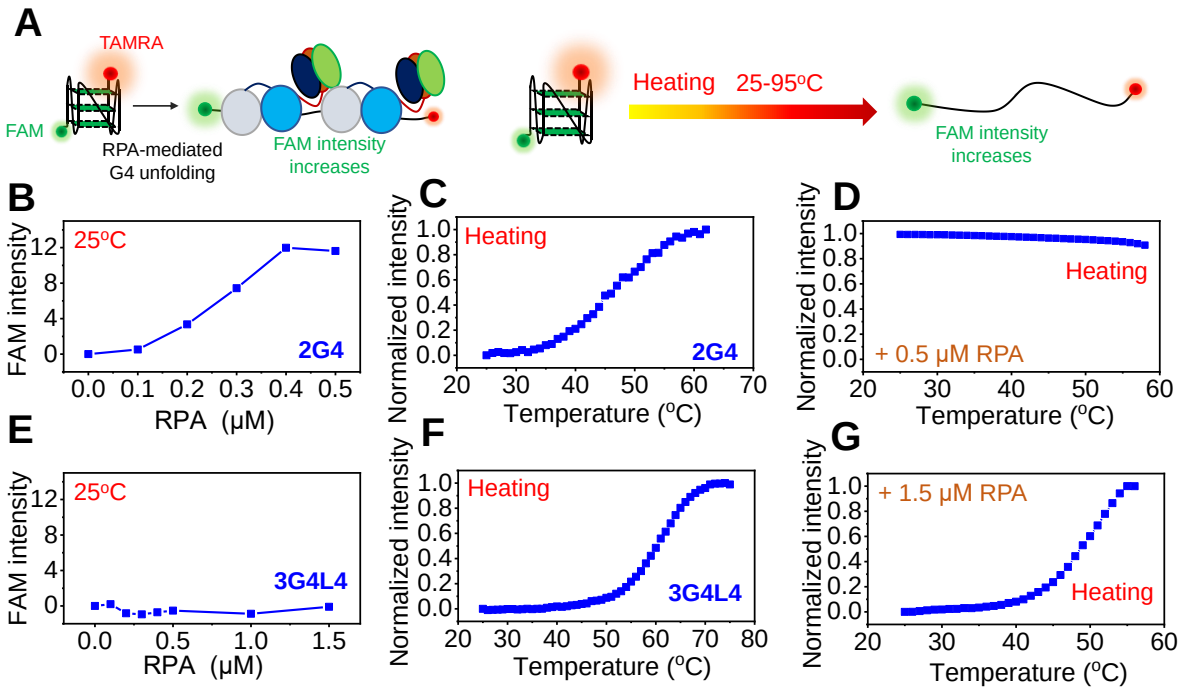

Figure S3. RPA significantly unfolds 2G4 in 100 mM KCl but has a poor destructive effect on the long-looped 3G4L4. Related to Figure 3. (A) The experimental design. First, we mixed G4s and RPA at room temperature for 5 min and the FAM intensity was recorded. Then we heated the sample from 25-95°C slowly. Due to the possible denaturation of RPA in the heating process, we only heated the sample from 25 °C to less than 60°C in the presence of proteins. G4 sequences were labeled with the FRET pairs FAM and TAMRA. FAM emission was low when G4s were well folded, and would increase once G4s were unfolded by proteins. Then in the FRET-melting assay, the unfolding of G4s during the heating process would also lead to increases in FAM intensity. **(B)** FAM intensity increases significantly with the addition of RPA, reflecting the unfolding of 2G4. The concentration of G4 in each experiment was 0.5 μM, and the FAM intensity reached the maximal value at 0.4-0.5 μM RPA. **(C-D)** FAM intensity of 2G4 increased during the heating process, indicating the unfolding of 2G4. However, there was no increase in FAM intensity during the heating when there was 0.5 μM RPA, further suggesting that the G4 structures were not folded at 25°C in the presence of RPA. **(E)** FAM intensity had no obvious change with the addition of 0-1.5 μM RPA, reflecting that 3G4L4 was not unfolded by RPA. **(F-G)** During the heating process, the FAM intensity of 3G4L4 increased, indicating the unfolding of G4 structures. The same trend can also be observed when there was 1.5 μM RPA, further suggesting that the G4 structures should be folded at 25°C in the presence of RPA.

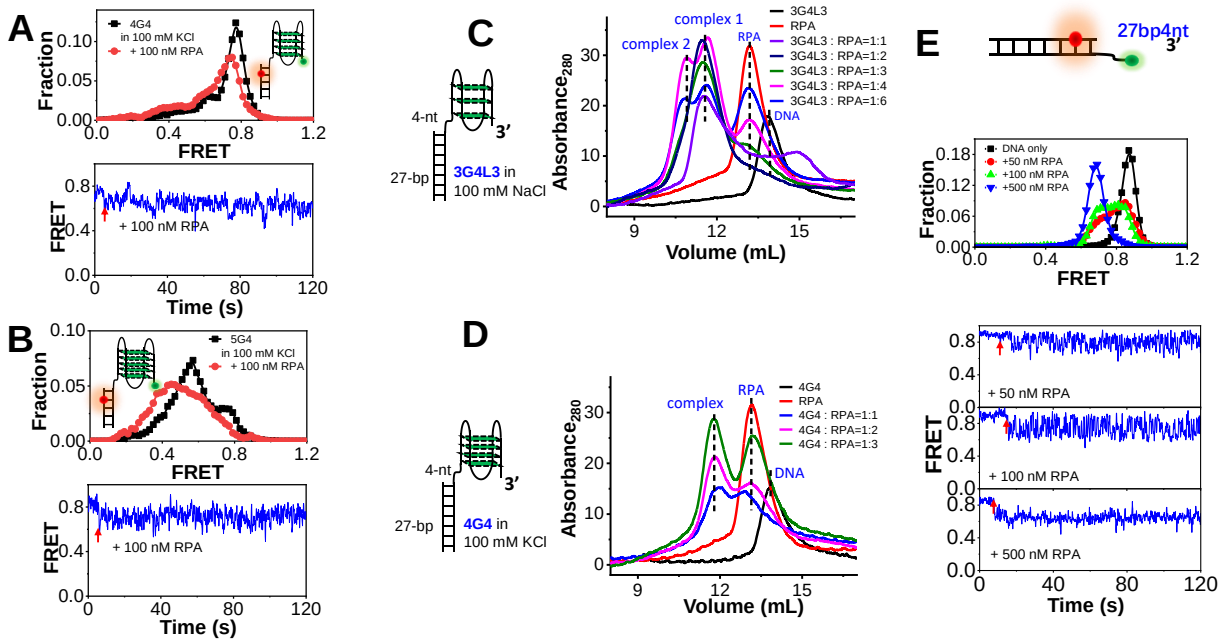

Figure S4. RPA may dynamically interact with the 4-nt linker between duplex DNA and the G4 structure. Related to Figure 3. (A) The 4-layered G4 DNA was poorly unfolded by RPA in 100 mM KCl. **(B)** The 5-layered G4 DNA was poorly unfolded by RPA in 100 mM KCl. (**C**) The gel filtration of complexes formed by RPA and 3G4L3 annealed in 100 mM NaCl. The x-axis is the elution volume, and the y-axis is the absorbance at 280 nm. There are two additional peaks besides free RPA and DNA, suggesting that RPA forms two types of complexes with 3G4L3 in 100 mM NaCl. (**D**) RPA forms only one type of complex with 4G4 annealed in 100 mM KCl. (**E**) RPA repetitively associates with and dissociates from 27bp4nt DNA in 100 mM KCl, 5 mM $MgCl_2$ with the FRET switching between ~$E_{0.9}$ and ~$E_{0.7}$.

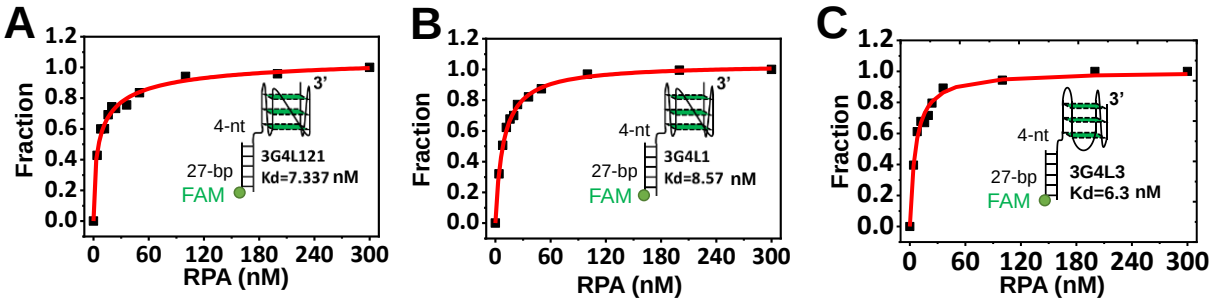

Figure S5. The equilibrium DNA-binding assay with RPA. Related to Figure 4. Both the G4 preparation and fluorescence anisotropy measurements were taken in 100 mM KCl, 5 mM $MgCl_2$. Each sample was allowed to equilibrate in the solution for 5 min, after which the fluorescence polarization was measured. The binding curve was fitted by the Hill equation: $y = [RPA]^n/(K_D^n+[RPA]^n)$, where y is the binding fraction, n is the Hill coefficient, and K_D is the apparent dissociation constant. RPA displays very similar affinities towards the substrates harboring 3G4L121 (**A**), 3G4L1 (**B**), and 3G4L3 (**C**) with the K_D values of 7.3, 8.6, and 6.3 nM. The n values are 0.90, 0.98, and 0.98. All the three n values are close to 1.0, reflecting that there is no significant cooperative binding of RPA.

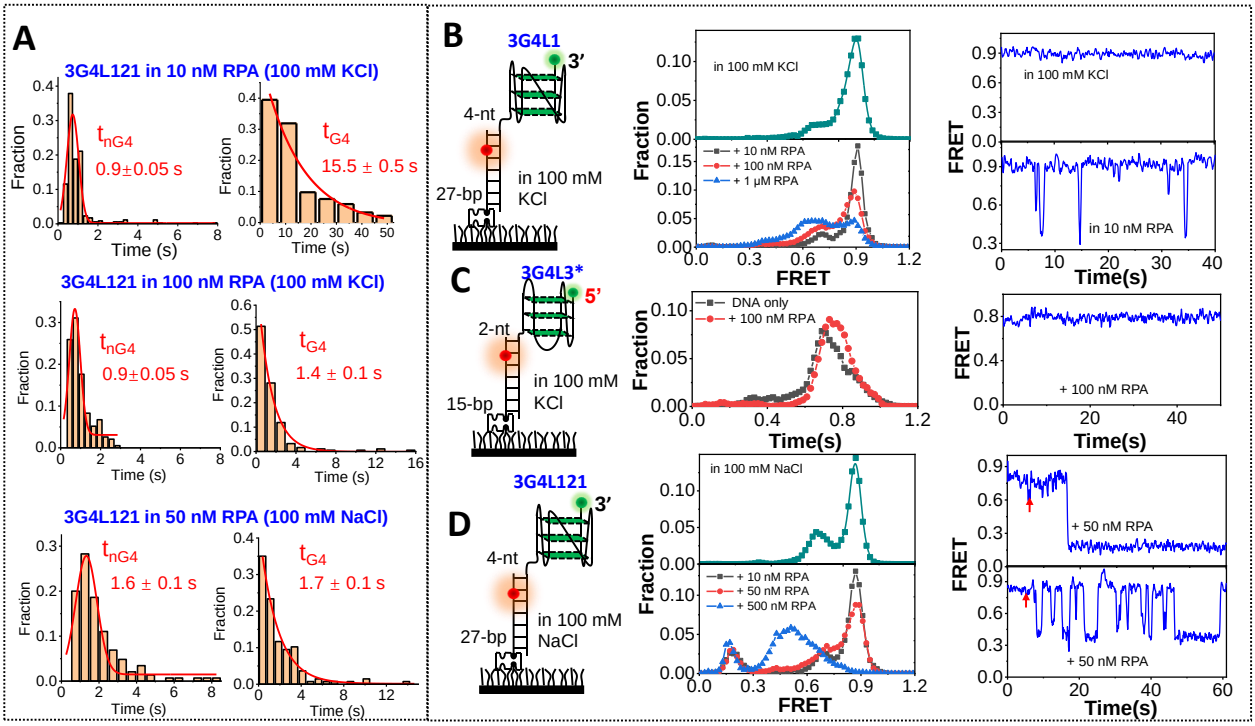

Figure S6. The interplay between RPA and G4s with short loops. Related to Figure 4. (A) The distributions of t_{nG4} and t_{G4} in 3G4L121 as shown in Figure 4C determined from about 100 single-molecule FRET traces in different conditions. The histograms of t_{nG4} were fitted by Gaussian distribution, and the histograms of t_{G4} were fitted by the exponential decay. **(B)** RPA is able to rapidly and transiently resolve the G4 structure with 1-nt loops. (**C**) The interaction of RPA with the G4 structures placed at the 5′-end of the duplex DNA in 100 mM KCl, 5 mM $MgCl_2$. 3G4L3* seldom shows FRET changes. **(D)** With the decreases in thermal stability in 100 mM NaCl compared with that in 100 mM KCl, more fractions of 3G4L121 molecules can be disrupted by RPA. The traces showing the stable FRET level at ~$E_{0.2}$, and the FRET decreases with longer duration time can be observed.

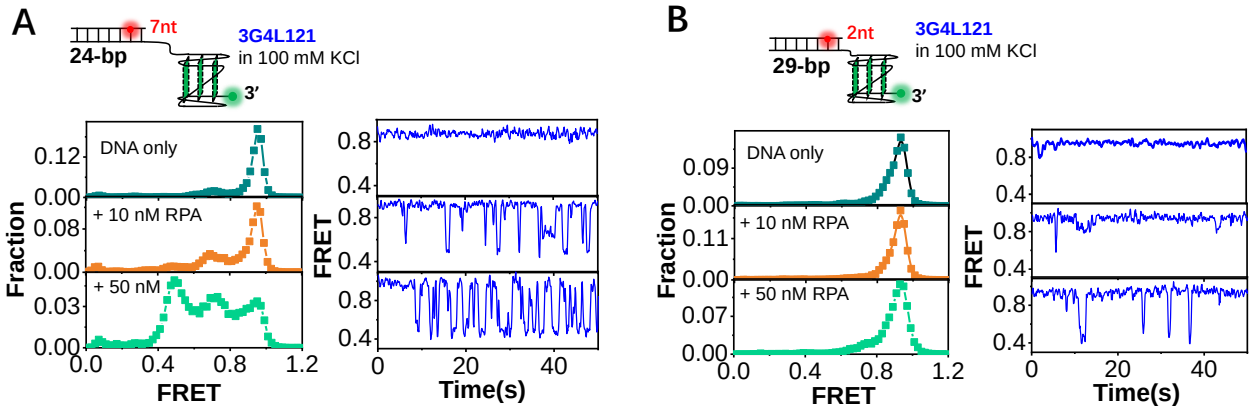

Figure S7. The influences of the DNA environment on the interaction between RPA and G4 DNA structure. Related to Figure 4. Increases (**A**) and decreases (**B**) in the linker length between duplex DNA and G4 structure leads to increases and decreases in the interaction frequency between RPA and G4, respectively. The t_{G4} of 3G4L121 in 50 nM RPA was determined to be ~2.1 s with the 7-nt linker and ~ 20 s with the 2-nt linker. The t_{nG4} were both ~ 1 s.

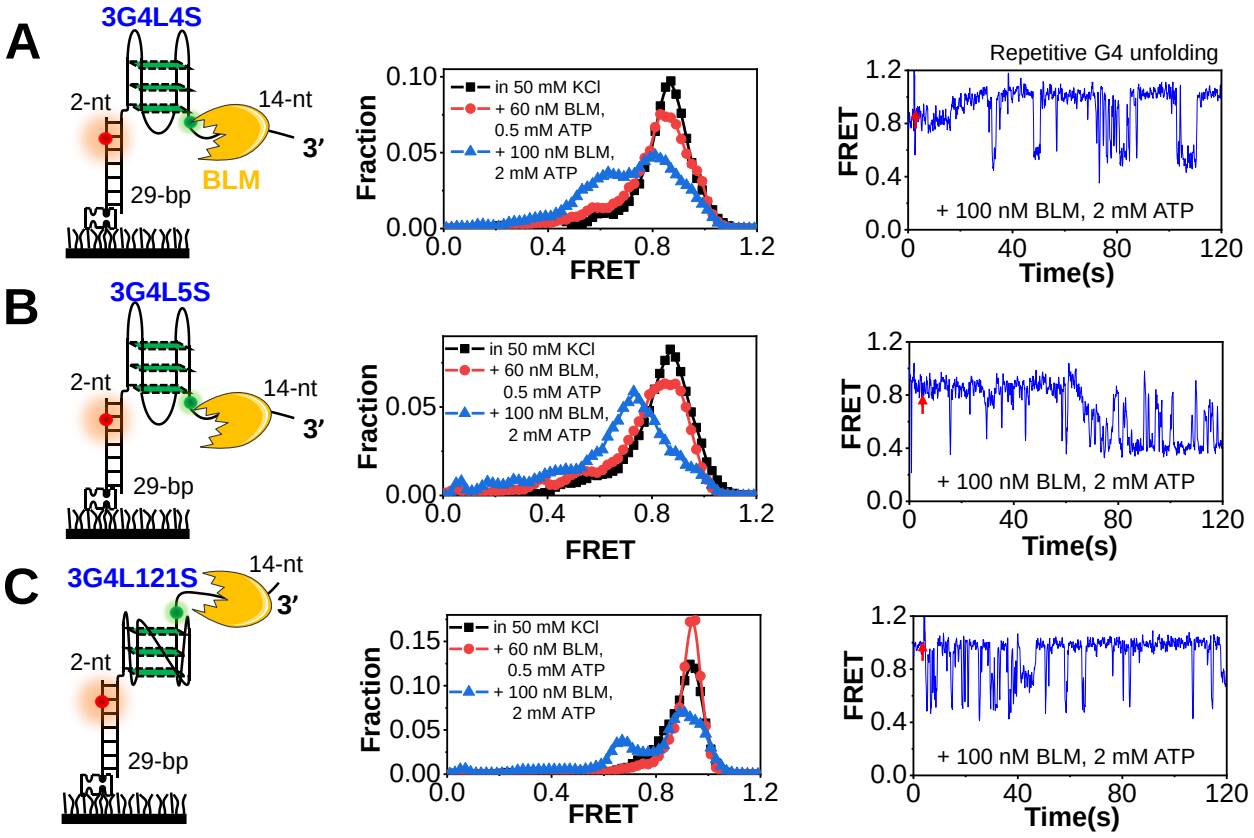

Figure S8. The BLM-mediated unfolding of G4 DNA structures with different loop lengths. Related to Figure 5. (A) FRET distributions of 3G4L4S before and after the addition of BLM, ATP, and the representative trace at 100 nM BLM, 2 mM ATP. **(B)** FRET distributions of 3G4L5S before and after the addition of BLM, ATP, and the representative trace at 100 nM BLM, 2 mM ATP. **(C)** FRET distributions of 3G4L121S before and after the addition of BLM, ATP, and the representative trace at 100 nM BLM, 2 mM ATP.

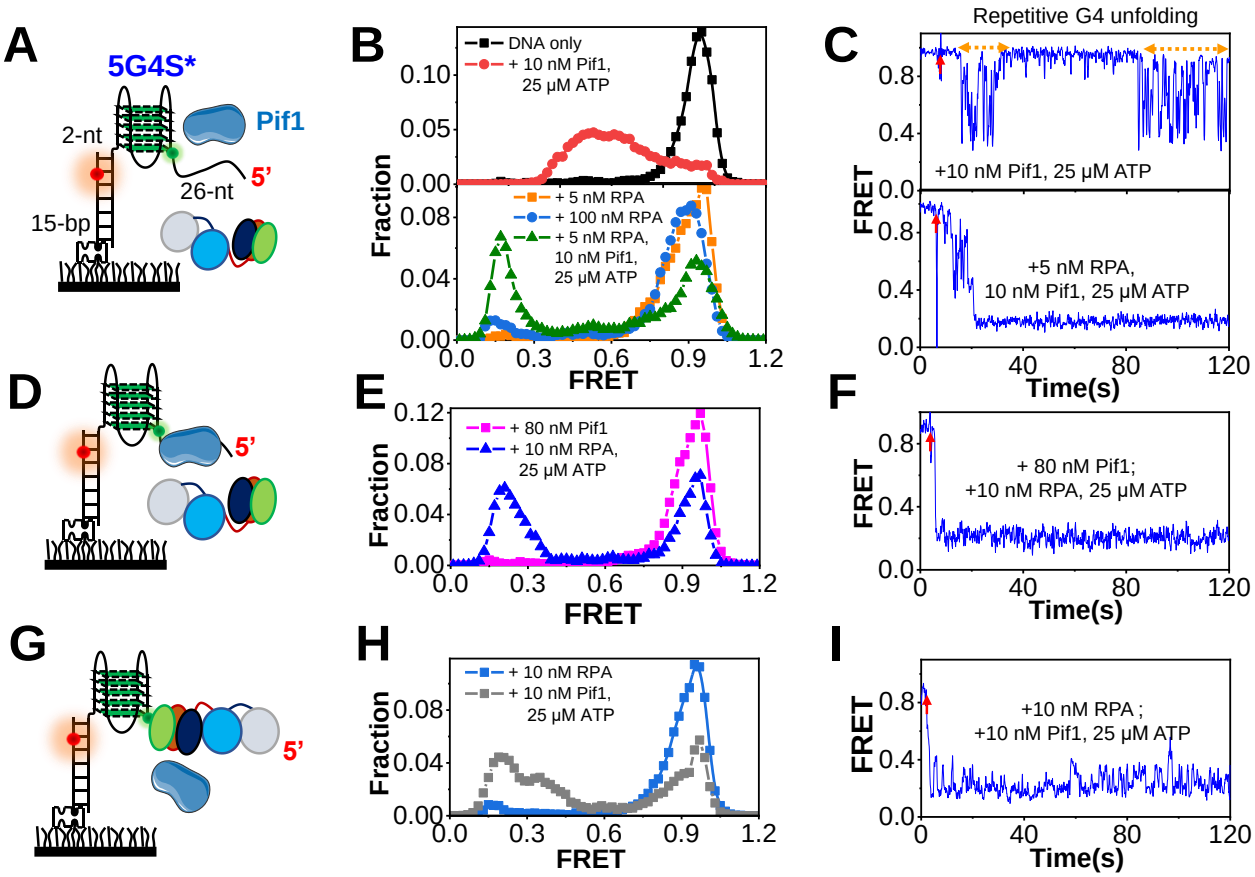

Figure S9. RPA promotes the stable unfolding of G4 structures in cooperation with Pif1 helicase. Related to Figure 6. (**A**) Schematic diagram of the 5-layered G4 DNA structure named 5G4S*. The unwinding buffer of 25 mM Tris-HCl, pH 7.5, 50 mM NaCl, and 5 mM $MgCl_2$ was used. (**B-C**) FRET distributions and traces in different conditions. (**D**) The experimental design that Pif1 was incubated with the substrate at first, and then RPA was introduced. **(E-F)** FRET distribution and trace before and after the addition of 25 μM ATP, 10 nM RPA to the Pif1-associated G4. **(G)** The experimental design that RPA was incubated with the substrate at first, then Pif1 and ATP were introduced. **(H-I)** FRET distribution and trace before and after the addition of 10 nM Pif1, 25 μM ATP to the RPA-associated G4.

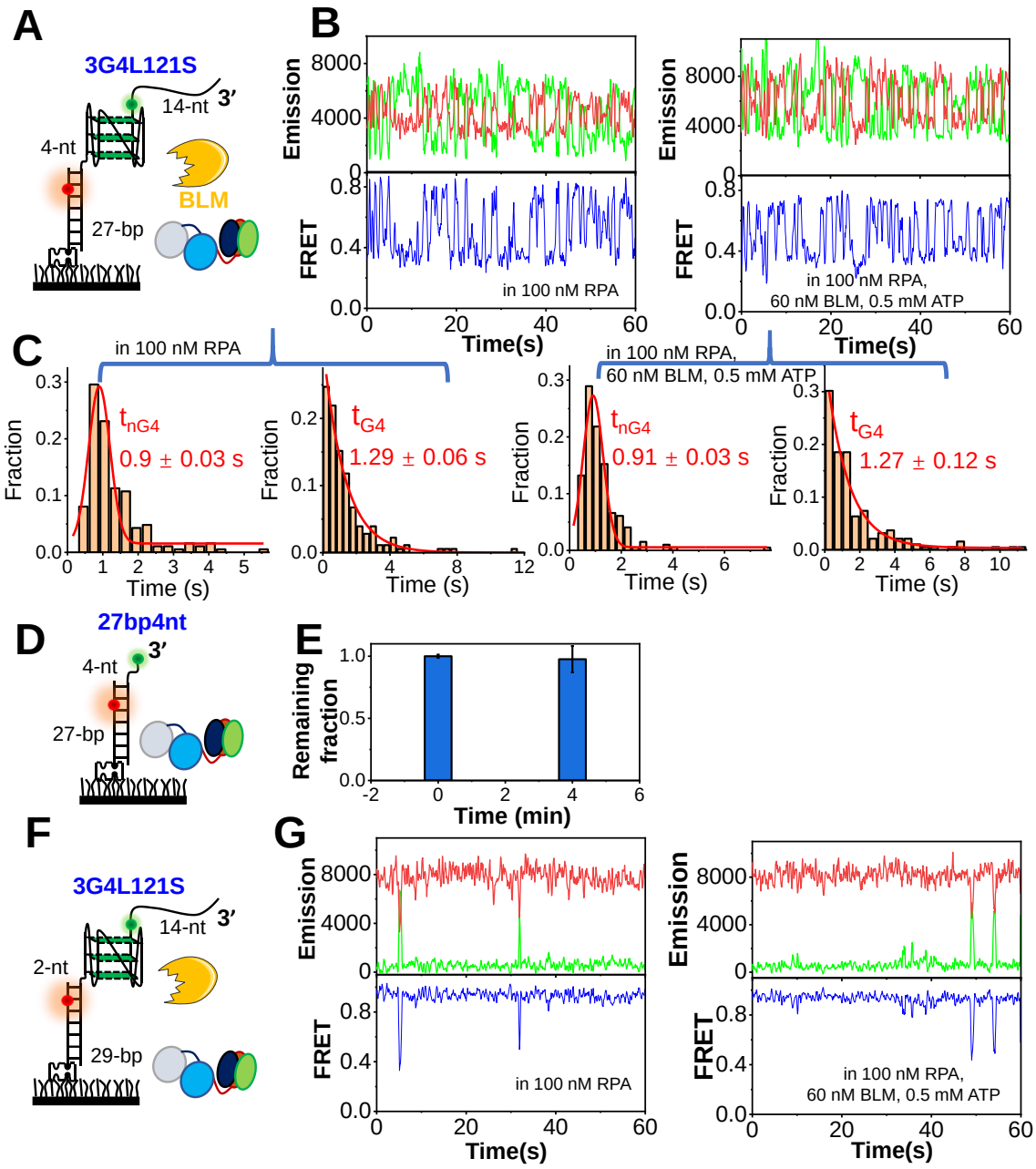

Figure S10. The interplay between RPA and BLM in the unfolding of short-looped G4. Related to Figure 7. (A) The schematic diagram of the 3G4L121S substrate. The ssDNA tail and duplex stem are 14-nt and 27-bp, respectively. There is a 4-nt linker between G4 and duplex. **(B)** Representative traces after the addition of 100 nM RPA, as well as the addition of 100 nM RPA, 60 nM BLM, and 0.5 mM ATP. **(C)** The distributions of t_{nG4} and t_{G4} in 3G4L121S in 100 nM RPA, and in 100 nM RPA, 60 nM BLM, 0.5 mM ATP. The histograms of t_{nG4} were fitted by Gaussian distribution, and the histograms of t_{G4} were fitted by the exponential decay. **(D)** The schematic diagram of the 27bp4nt substrate. The ssDNA tail and duplex stem are 4-nt and 27-bp, respectively. **(E)** The remaining fractions of 27bp4nt on coverslip before and 4 minutes after the addition of 100 nM RPA, 60 nM BLM, 0.5 mM ATP. The error bars were obtained from at least three repetitive experiments. Data are presented as mean±SEM. **(F)** There is a 2-nt linker between G4 and duplex. **(G)** Representative traces after the addition of 100 nM RPA, and 100 nM RPA, 60 nM BLM, 0.5 mM ATP.

Table S1. DNA sequences used in this study. Related to Figures 1-7.

Names	Sequences（5’-3’）
	Sequences (5’-3’) of substrates for single-molecule FRET
2G4	GCGTGGCACCGGTAATAGGAAATAGGAGATT**GGTTGGTGTGGTTGG**TT-Cy3
3G4L1	GCGTGGCACCGGTAATAGGAAATAGGAGATT**GGGTGGGTGGGTGGG**TT-Cy3
3G4L121	GCGTGGCACCGGTAATAGGAAATAGGAGATT**GGGTGGGTAGGGTGGG**TT-Cy3
3G4L2	GCGTGGCACCGGTAATAGGAAATAGGAGATT**GGGTTGGGTTGGGTTGGG**TT-Cy3
3G4L3	GCGTGGCACCGGTAATAGGAAATAGGAGATT**GGGTTAGGGTTAGGGTTAGGG**TT-Cy3
3G4L4	GCGTGGCACCGGTAATAGGAAATAGGAGATT**GGGTTTTGGGTTTTGGGTTTTGGG**TT-Cy3
3G4L5	GCGTGGCACCGGTAATAGGAAATAGGAGATT**GGGTTTTTGGGTTTTTGGGTTTTTGGG**TT-Cy3
4G4	GCGTGGCACCGGTAATAGGAAATAGGAGATT**GGGGTGTGGGGACAGGGGTGTGGGG**TT-Cy3
4G4*	GCGTGGCACCGGTAATAGGAAATAGGAGATT**GGGGTTAGGGGTTAGGGGTTAGGGG**TT-Cy3
5G4	GCGTGGCACCGGTAATAGGAAATAGGAGATT**GGGGGTTAGGGGGTTAGGGGGTTAGGGGG**TT-Cy3
27bp4nt	GCGTGGCACCGGTAATAGGAAATAGGAGATT-Cy3
3G4L121S	GCGTGGCACCGGTAATAGGAAATAGGAGATT**GGGTGGGTAGGGTGGG**TT(iCy3)ACACCAAGAAGT
3G4L3S	GCGTGGCACCGGTAATAGGAAATAGGAGATT**GGGTTAGGGTTAGGGTTAGGG**TT(iCy3)TTTTTTTTTTT
3G4L4S	GCGTGGCACCGGTAATAGGAAATAGGAGATT**GGGTTTTGGGTTTTGGGTTTTGGG**TT(iCy3)TTTTTTTTTTT
3G4L5S	GCGTGGCACCGGTAATAGGAAATAGGAGATT**GGGTTTTTGGGTTTTTGGGTTTTTGGG**TT(iCy3)TTTTTTTTTTT
Stem1(27 nt)	TCCTAT(iCy5)TTCCTATTACCGGTGCCACGC-Biotin
Stem2(29 nt)	TCTCCT(iCy5)ATTTCCTATTACCGGTGCCACGC-Biotin
Stem3(24 nt)	Cy5-TATTTCCTATTACCGGTGCCACGC-Biotin
3G4L121*	Cy3-**GGGTGGGTAGGGTGGG**ATGTATGACAAGGAAGG
3G4L3*	Cy3-**GGGTTAGGGTTAGGGTTAGGG**ATGTATGACAAGGAAGG
5G4S*	AAGCAGTGGTATCAACGCAGAGAAAT(iCy3)**GGGGGTAGGGGGTAGGGGGTAGGGGG**ATGTATGTCAAGGAAGG
3G4L121S*	AAGCAGTGGTATCAACGCAGAGAAAT(iCy3)**GGGTGGGTAGGGTGGG**ATGTATGTCAAGGAAGG
3G4L4S*	AAGCAGTGGTATCAACGCAGAGAAAT(iCy3)**GGGTTTTGGGTTTTGGGTTTTGGG**ATGTATGTCAAGGAAGG
15bp2nt	Cy3-ATGTATGTCAAGGAAGG
Stem (15 nt)	Biotin-CCTTCCTTGT(iCy5)CATAC
	Sequences (5’-3’) of substrates for FRET Melting
2G4	FAM-TGG*TT*GG*TGT*GG*TT*GGT-TAMRA
3G4L1	FAM-TGGG*T*GGG*T*GGG*T*GGGT-TAMRA
3G4L121	FAM-TGGG*T*GGG*TA*GGG*T*GGGT-TAMRA
3G4L2	FAM-TGGG*TT*GGG*TT*GGG*TT*GGGT-TAMRA
3G4L3	FAM-TGGG*TTA*GGG*TTA*GGG*TTA*GGGT-TAMRA
3G4L4	FAM-TGGG*TTTT*GGG*TTTT*GGG*TTTT*GGGT-TAMRA
3G4L5	FAM-TGGG*TTTTT*GGG*TTTTT*GGG*TTTTT*GGGT-TAMRA
4G4	FAM-TGGGG*TGT*GGGG*ACA*GGGG*TGT*GGGGT-TAMRA
5G4	FAM-TGGGGG*TTA*GGGGG*TTA*GGGGG*TTA*GGGGGT-TAMRA
	Sequences (5’-3’) of substrates for CD
2G4	GG*TT*GG*TGT*GG*TT*GG
3G4L1	GGG*T*GGG*T*GGG*T*GGG
3G4L121	GGG*T*GGG*TA*GGG*T*GGG
3G4L2	GGG*TT*GGG*TT*GGG*TT*GGG
3G4L3	GGG*TTA*GGG*TTA*GGG*TTA*GGG
3G4L4	GGG*TTTT*GGG*TTTT*GGG*TTTT*GGG
3G4L5	GGG*TTTTT*GGG*TTTTT*GGG*TTTTT*GGG
4G4*	GGGG*TTA*GGGG*TTA*GGGG*TTA*GGGG
4G4	GGGG*TGT*GGGG*ACA*GGGG*TGT*GGGG
5G4	GGGGG*TTA*GGGGG*TTA*GGGGG*TTA*GGGGG
	Sequences (5’-3’) of substrates for Equilibrium DNA-binding assay
3G4L1	GCGTGGCACCGGTAATAGGAAATAGGAGATT**GGGTGGGTGGGTGGG**TT
3G4L121	GCGTGGCACCGGTAATAGGAAATAGGAGATT**GGGTGGGTAGGGTGGG**TT
3G4L3	GCGTGGCACCGGTAATAGGAAATAGGAGATT**GGGTTAGGGTTAGGGTTAGGG**TT
Stem	TCCTATTTCCTATTACCGGTGCCACGC-FAM

The internal fluorophores were labeled on the base Thymine. The underline indicates the sequence to form duplex DNA with the complementary strand.

Table S2. T_m values of G4 structures were obtained from the FRET-melting assay. Related to Figures 1-7.

	2 mM NaCl	10 mM NaCl	20 mM NaCl	50 mM NaCl	100 mM NaCl	200 mM NaCl	2 mM KCl	10 mM KCl	20 mM KCl	50 mM KCl	100 mM KCl	200 mM KCl
2G4	-	42.7	43.4	44.8	46.8	47.8	43.4	45.3	47.1	48.0	50.2	52.7
3G4L1	52.5	52.5	56.5	57.7	63.0	68.1	67.7	80.4	85.1	>92.7	>94.9	>95.4
3G4L121	48.8	49.7	49.7	52.8	57.4	62.1	57.4	70.3	76.0	>84.2	>87.7	>89.4
3G4L2	47.9	48.1	48.3	49.4	50.3	52.9	49.7	54.4	60.4	67.4	72.0	75.7
3G4L3	44.7	44.9	45.0	46.2	49.6	54.6	45.8	51.8	56.5	62.4	66.8	71.0
3G4L4	40.7	42.4	42.6	42.6	43.3	46.6	41.7	46.1	50.9	56.9	61.1	65.5
3G4L5	-	-	-	-	42.0	44.4	40.0	42.3	45.8	50.4	54.0	57.7
4G4	50.3	50.5	51.9	56.6	61.9	67.3	68.6	80.8	85.3	>92.9	>94.6	>95
5G4	53.1	54.4	57.4	64.6	70.9	76.4	71.5	84.6	>89.4	>94.3	>95	>95

The values are the T_m at the indicated concentration of NaCl or KCl, and 5 mM $MgCl_2$.

- denotes that the T_m cannot be determined.

Table S3. The number of FRET traces used in the FRET distributions. Related to Figures 1-7.

		25 mM Tris HCl	+200 mM KCl	+10 nM RPA	+50 nM RPA	+100 nM RPA	+500 nM RPA
Figure 1B-G	3G4L1	425	396	398	394	390	402
	3G4L121	385	365	369	385	350	332
	3G4L2	485	452	490	425	433	462
	3G4L3	501	485	456	442	469	423
	3G4L4	462	450	426	416	415	434
	3G4L5	389	365	374	358	355	376
	5G4	399	376	385	379	369	371
Figure S2A-D	4G4*	416	402	415	398	395	386
	4G4	501	486	475	459	426	450
	2G4	398	380	375			
Figure 3B-F	2G4	100 mM KCl 551	+ 10 nM RPA 542				
	3G4L3	100 mM NaCl 432	+ 10 nM RPA 421	100 mM KCl 521	+ 100 nM RPA 515		
	3G4L4	100 mM KCl 677	+ 100 nM RPA 696				
	3G4L5	100 mM KCl 433	+ 100 nM RPA 436				
Figure S4	4G4	100 mM KCl 365	+ 100 nM RPA 350				
	5G4	100 mM KCl 387	+ 100 nM RPA 344				
	27bp4nt	100 mM KCl 402	+ 50 nM RPA 396	+ 100 nM RPA 387	+ 500 nM RPA 389		
Figure 4B, E	3G4L121	100 mM KCl 410	+ 10 nM RPA 377	+ 100 nM RPA 361	+ 1 μM RPA 349		
	3G4L121*	100 mM KCl 385	+ 100 nM RPA 347				
Figure S6	3G4L1	100 mM KCl 445	+ 10 nM RPA 465	+ 100 nM RPA 491	+ 1 μM RPA 523		
	3G4L3*	100 mM KCl 493	+ 100 nM RPA 491				
	3G4L121	100 mM NaCl 458	+ 10 nM RPA 442	+ 50 nM RPA 481	+ 500 nM RPA 432		
Figure S7	3G4L121(7 nt)	100 mM KCl 362	+ 10 nM RPA 350	+ 50 nM RPA 351			
	3G4L121(2 nt)	100 mM KCl 506	+ 10 nM RPA 467	+ 50 nM RPA 465			
Figure 5	3G4L3S	DNA only 652	+ 40 nM BLM 640	+ BLM, ATP 625			
	3G4L4S*	DNA only 739	+ 40 nM Pif1 725	+ Pif1, ATP 387			
	3G4L121S*	DNA only 452	+ 80 nM Pif1, ATP 421				
Figure S8	3G4L4S	DNA only 703	+ 60 nM BLM 644	+ 100 nM BLM 635			
	3G4L5S	DNA only 401	+ 60 nM BLM 395	+ 100 nM BLM 382			
	3G4L121S	DNA only 433	+ 60 nM BLM 367	+ 100 nM BLM 314			

Figure 6B	3G4L3S	+10 nM RPA 460	+20 nM RPA 421	+40 nM RPA 403	+80 nM RPA 405	+10 nM RPA, 40 nM BLM 396
Figure S9B	5G4S*	DNA only 447	+10 nM Pif1, ATP 430	+5 nM RPA 425	+100 nM RPA 370	+5 nM RPA, Pif1,ATP 401
S9E	5G4S*	+80 nM Pif1 452	+10 nM RPA, ATP 430			
S9H	5G4S*	+10 nM RPA 425	+10 nM Pif1, ATP 406			
Figure 7C	3G4L121S	DNA only 468	+ 100 nM RPA 423	+ 100 nM RPA, BLM, ATP 181		